Generalized H-infinity Vehicle Control Utilizing Dimensional Analysis

S. Brennan *A. Alleyne**

Dept. of Mechanical & Industrial Engineering

University of Illinois at Urbana-Champaign

1206 W. Green Street, Urbana, IL 61801

**corresponding author*

ABSTRACT

The selection of a nominal plant model is a central design choice for a robust controller design. In the case of vehicle dynamic studies, the nominal plant model for a vehicle is traditionally chosen using knowledge of a particular experimental vehicle under study. With such a design focus on one particular plant, it may be questionable whether the resulting controller synthesis technique provides experimental conclusions that are generalizable to several other vehicle types. This work develops an alternative, dimensionless representation of vehicle dynamics that is more suitable for a generalized vehicle analysis. Within such a nondimensional framework, the average of vehicle parameters becomes well defined, and perturbations about the average are easily developed that reasonably encompass all production vehicles. These uncertainty bounds are then used to generate a robust controller suitable for nearly all passenger vehicles. For the purposes of demonstration, the focus of this work is a lateral-positioning control task. The resulting controller is demonstrated on a scaled experimental vehicle.

1. PREVIOUS WORK AND PROBLEM STATEMENT

Robust controller design techniques have been applied to the field of vehicle chassis control to achieve many different performance objectives: robust yaw rate control [1,2], robust lateral positioning using one [2, 3] or more driver inputs [4-6]. A difficulty with many published approaches is to obtain an adequate description of the model uncertainty. Most descriptions depend on plant frequency responses or parameter perturbations with a single vehicle under consideration. The resulting controller design is therefore often vehicle specific, i.e. suitable only for application to a single design vehicle.

This work seeks to develop a more general representation of vehicle controllers so that one controller is implementable on any production vehicle. Because production vehicles span a large range in size and mass, a novel, size-independent method of model representation and controller design is necessary. For purposes of demonstration, the familiar task of positioning the vehicle laterally at high speed on a nominal highway surface was chosen. This task was considered earlier in [3] and [7] using an LMI and stacked sensitivity approach, respectively. While both controller designs were robust to vehicle-to-vehicle model variations, each had limitations. The first did not account for unmodeled dynamics other than parameter variation, while the second exhibited poor transient performance. Both of these aspects are improved upon in the current design.

This paper is summarized as follows: Section 2 presents distributions of vehicle parameters and a discussion of methods of discovering outliers. Section 3 presents equations for the linear, lateral vehicle dynamics with a fixed preview distance. Section 4 defines the robustness criteria required for generalized vehicle control: that a controller must stabilize the average vehicle dynamics in the presence of perturbations that generate the range of published vehicle dynamics. Section 5 develops a robust controller design to demonstrate a single-velocity robust controller implementation. Section 6 presents simulation and experimental results. Finally, a discussion and conclusion summarizes the primary findings.

2. PARAMETER DISTRIBUTIONS

Motivating the nondimensional representation is the desire to develop controller implementations suitable to any vehicle. Consequently, vehicle-to-vehicle variation is addressed in a dimensionless framework that utilizes the Buckingham Pi theorem [8]. The resulting representation accommodates two modeling aspects previously ignored by other researchers: first, parameter-to-parameter interdependency clearly arises due to common vehicle design; second, the individual parameter distributions show normal distributions in the nondimensional representation that provide a numerically well-defined mean and standard deviation of vehicle dynamics [3, 9].

Application of the Buckingham Pi theorem [8] to the classical vehicle dynamics known as the Bicycle Model yields new, dimensionless groupings of parameters that collectively do not have dimensions. These dimensionless groupings are known as pi parameters, and represent a reparameterization of the problem in a unit- or dimension-independent framework (see [10] for further details). For the planar bicycle model these parameters are:

$$\pi_1 = \frac{a}{L}, \pi_2 = \frac{b}{L}, \pi_3 = \frac{C_{\alpha f} \cdot L}{mU^2}, \pi_4 = \frac{C_{\alpha r} \cdot L}{mU^2}, \pi_5 = \frac{I_z}{mL^2} \tag{1}$$

With:

Proceedings of the American Control Conference
Denver, Colorado June 4-6, 2003

m = vehicle mass (5.451 kg)
I_z = vehicle moment of inertia (0.1615 kgm^2)
V = vehicle longitudinal velocity (3.0 m/s)
a = distance from C.G. to front axle (0.1461 m)
b = distance from C.G. to rear axle (0.2191 m)
L = vehicle length, a + b (0.3652 m)
$C_{\alpha f}$ = cornering stiffness of front 2 tires (65 N/rad)
$C_{\alpha r}$ = cornering stiffness of rear 2 tires (110 N/rad)

The values in parenthesis are quite different from a typical full-sized vehicle because they correspond to the measured values for a 1/7-scale experimental scale used on the Illinois Roadway Simulator, a treadmill/vehicle counterpart to a wind tunnel/airplane testing system. The similarity in dynamics between this vehicle and full-sized vehicles was proven via the Buckingham-Pi Theorem, and was the original motivation for analyzing vehicle dynamics in a nondimensional framework. Derivation and explanations of the vehicle Π parameters are given in more detail in [9]. Note that a vehicle model described by *vehicle-mLU* dimensions has reduced parametric dependence, from 8 dimensional parameters to 5 nondimensional parameters. Further, π_2 is not independent and can be obtained by definition:

$$\pi_2 = 1 - \pi_1 \tag{2}$$

so that there are only 4 descriptive, primary parameters for each vehicle instead of the 8 normally associated with bicycle-model vehicle dynamics.

The similarity in dynamics between systems relies on comparisons between different pi parameters, a concept proven via the Buckingham-Pi Theorem nearly 100 years ago [8]. This Theorem is traditionally utilized used to compare two dissimilarly-sized systems: if two systems have equivalent pi-parameters, then they are dimensionally similar and a transform exists that will map behavior of one system directly to the other. Additionally, the numerical 'closeness' of two systems with regard to their pi-parameters is a very fundamental measure of the closeness of two systems dynamically, a metric that is independent of the units of measurement or the linearity/nonlinearity of the governing dynamics. Therefore, the reparameterization of vehicle dynamics to nondimensional coordinates is quite useful in the comparison of different vehicles.

Another improvement of this work over previous studies is the careful exclusion of vehicle measurements that are outliers in the distribution of pi parameters. To find such outliers, additional vehicle measurements were obtained from the National Highway Safety and Transportation Administration (NHTSA) [11]. These measurements did not contain tire cornering stiffness values, so only the π_1, π_2, and π_5 parameters can be calculated. However, these are sufficient to reveal several vehicles that were outliers in the original data. This is seen clearly in Fig. 1 below, where the parameters from the previous study (dark) and data from the NHTSA crash testing database (light) are shown.

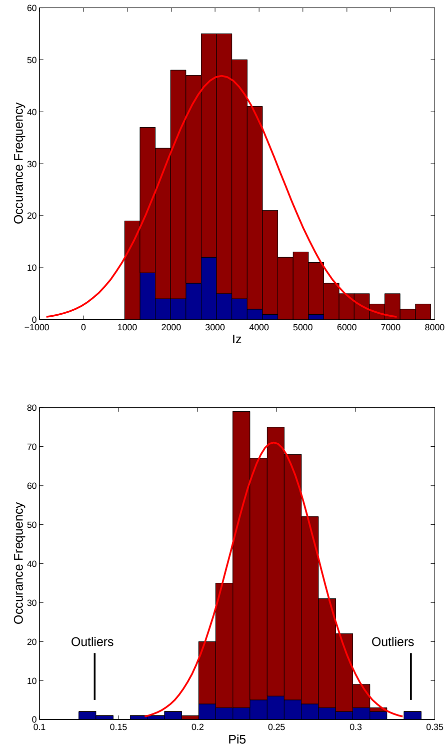

Fig. 1: Outliers are not obvious in the dimensional (top) distributions, but are obvious in the nondimensional (bottom) distributions of the same parameter

One problem with using traditional, dimensioned parameters to define a model for robust controller design is that the mean and range of production vehicle dynamics are difficult to define; their distribution is non-normal and highly skewed (top plot of Fig. 1). For the dimensional parameter, I_z, to fit to a 2-standard-deviation guassian distribution about the average, vehicles with *negative* inertia would be required. A relative distribution of the corresponding nondimensional vehicle π_5 parameter shows a much more normal trend, seen in the bottom plot of the same figure. Clearly, the nondimensional distribution is more amenable to a definition of an average parameter as well as operating parameter range. Distributions of the remaining three pi-parameters with the outliers removed are shown below for the collection of full-size vehicle parameters discussed earlier. Note that the two velocity-dependent parameters, π_3 and π_4, are calculated for a fixed speed of 28 m/s. Because the NHTSA data does not include cornering stiffnesses, the π_3 and π_4 datasets are much smaller. Also, by Equation (1) the π_3 and π_4 parameters are strongly dependent upon longitudinal speed, but the *ratio* of π_3 to π_4 is speed independent.

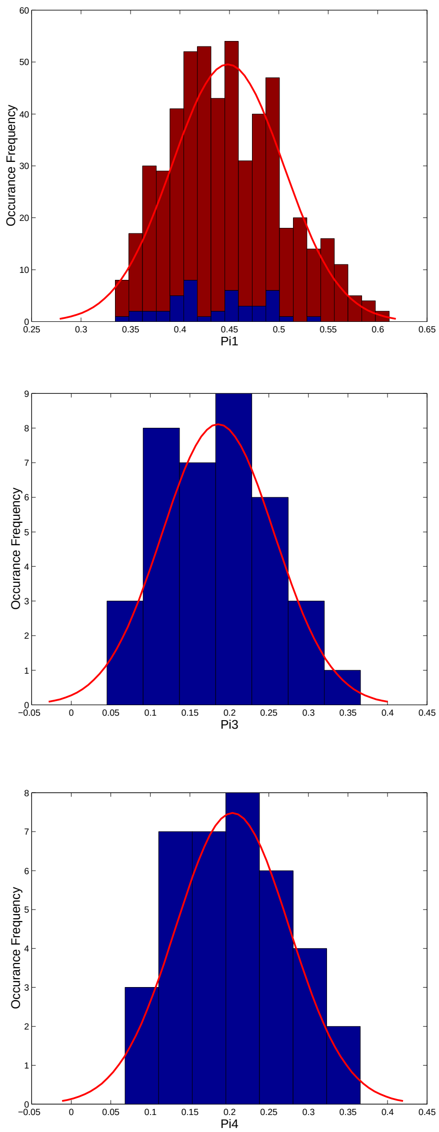

Fig. 2: Distribution of Pi parameters

From the distributions of Fig. 2, the average pi parameters are obtained for full-sized production vehicles:

$$\bar{\pi}_1 = 0.4431, \bar{\pi}_3 = \frac{145.6771}{\mathrm{U}^2}, \bar{\pi}_4 = 1.0977 \cdot \bar{\pi}_3, \bar{\pi}_5 = 0.2510 \tag{3}$$

These average values provide the dynamics of an average vehicle when substituted into the bicycle model, which is discussed shortly.

3. VEHICLE DYNAMICS

The space description of vehicle dynamics is based on the bicycle model [12] with the state vector [lateral position, lateral velocity, yaw angle, yaw rate]:

$$\mathbf{x} \equiv \begin{bmatrix} y & \frac{dy}{dt} & \psi & \frac{d\psi}{dt} \end{bmatrix}^T \tag{4}$$

and front steering input, $\mathbf{u} \equiv \left[\delta_f\right]^T$, as the sole control channel. Note that all states are measured with respect to the vehicle's center-of-gravity. The state space representation (in path error coordinates) [12] is:

$$\frac{d\mathbf{x}}{dt} = \mathbf{A} \cdot \mathbf{x} + \mathbf{B} \cdot \mathbf{u}, \mathbf{y} = \mathbf{C} \cdot \mathbf{x} \tag{5}$$

with:

$$\mathbf{A} = \begin{bmatrix} 0 & 1 & 0 & 0 \\ 0 & -\frac{f_1}{mU} & \frac{f_1}{m} & \frac{-f_2}{mU} \\ 0 & 0 & 0 & 1 \\ 0 & \frac{-f_2}{I_z \cdot U} & \frac{f_2}{I_z} & \frac{-f_3}{I_z \cdot U} \end{bmatrix}, \mathbf{B} = \begin{bmatrix} 0 \\ \frac{C_{\alpha f}}{m} \\ 0 \\ \frac{a \cdot C_{\alpha f}}{I_z} \end{bmatrix}, \mathbf{C} = \begin{bmatrix} 1 \\ 0 \\ 0 \\ 0 \end{bmatrix}^T \tag{6}$$

$$f_1 = C_{\alpha f} + C_{\alpha r}, f_2 = a \cdot C_{\alpha f} - b \cdot C_{\alpha r}, f_3 = a^2 \cdot C_{\alpha f} + b^2 \cdot C_{\alpha r}$$

The non-dimensionalization transforms are obtained by a state substitution that normalizes each state with respect to distance, mass, and time. The same approach was used to generate the parameters of Equation (1). As with any unit-independent representation, the nondimensional dynamics can be rewritten entirely in terms of the Π parameters. Mathematically, this is shown via a variable substitution defined by:

$$\mathbf{x} = \mathbf{M} \cdot \mathbf{x}^* \tag{7}$$

The above state normalizations are combined with a time normalization, $t = \mathbf{S} \cdot t^*$. For the vehicle system, $\mathbf{S} = \frac{L}{U}$, and $\mathbf{M}$ is defined as:

$$\mathbf{M} = diag\begin{bmatrix} L & U & 1 & \frac{U}{L} \end{bmatrix} \tag{8}$$

The state-space equations can be rewritten in the states $\mathbf{x}^*$ and time unit t^* as:

$$\frac{d\mathbf{x}}{dt} = \frac{d\left(\mathbf{M} \cdot \mathbf{x}^*\right)}{dt} = \frac{1}{\mathbf{S}} \cdot \mathbf{M} \cdot \frac{d\mathbf{x}^*}{dt^*} \tag{9}$$

We also assume that the input and output satisfy the dimensional mappings:

$$\mathbf{u} = \mathbf{U} \cdot \mathbf{u}^* \tag{10}$$

$$\mathbf{y} = \mathbf{Y} \cdot \mathbf{y}^* \tag{11}$$

Substitution gives:

$$\begin{aligned} \frac{d\mathbf{x}^*}{dt^*} &= \mathbf{SM}^{-1}\mathbf{AM} \cdot \mathbf{x}^* + \mathbf{SM}^{-1}\mathbf{BU} \cdot \mathbf{u}^* \\ \mathbf{y}^* &= \mathbf{Y}^{-1}\mathbf{CM} \cdot \mathbf{x}^* + \mathbf{Y}^{-1}\mathbf{DU} \cdot \mathbf{u}^* \end{aligned} \tag{12}$$

An equivalent nondimensional system can then be made of the form:

$$\begin{aligned} \dot{\mathbf{x}}^* &= \mathbf{A}^* \mathbf{x}^* + \mathbf{B}^* \mathbf{u}^* \\ \mathbf{y}^* &= \mathbf{C}^* \mathbf{x}^* + \mathbf{D}^* \mathbf{u}^* \end{aligned} \tag{13}$$

as long as the state space matrices satisfy (by inspection):

$$\begin{aligned} \mathbf{A}^* &= \mathbf{SM}^{-1}\mathbf{AM}, \quad \mathbf{B}^* = \mathbf{SM}^{-1}\mathbf{BU} \\ \mathbf{C}^* &= \mathbf{Y}^{-1}\mathbf{CM}, \quad \mathbf{D}^* = \mathbf{Y}^{-1}\mathbf{DU} \end{aligned} \tag{14}$$

Giving:

$$\mathbf{A}^* = \begin{bmatrix} 0 & 1 & 0 & 0 \\ 0 & -p_1 & p_1 & -p_2 \\ 0 & 0 & 0 & 1 \\ 0 & \frac{-p_2}{\Pi_5} & \frac{p_2}{\Pi_5} & \frac{-p_3}{\Pi_5} \end{bmatrix}, \quad \mathbf{B}^* = \begin{bmatrix} 0 \\ \Pi_3 \\ 0 \\ \frac{\Pi_1 \cdot \Pi_3}{\Pi_5} \end{bmatrix} \tag{15}$$

$$p_1 = \Pi_3 + \Pi_4, p_2 = \Pi_1\Pi_3 - \Pi_2\Pi_4, p_3 = \Pi_1^2\Pi_3 + \Pi_2^2\Pi_4$$

A similar non-dimensionalization can be obtained in the Laplace domain, generating transfer function dynamics solely dependent on the vehicle Π parameters.

In previous work [7], an error preview method was used [13-15] to make the control problem more amenable. In this work, the same method is utilized with a modification that the preview distance be a fixed 2 lengths of the vehicle. Under this constraint, the **C*** matrix becomes:

$$\mathbf{C}^* = \begin{bmatrix} 1 & 0 & 2 & 0 \end{bmatrix}. \tag{16}$$

This form of the output matrix is different from the previous study [7], where a fixed preview time of 2 seconds was selected. A 2-second preview time at high-speeds corresponds to a 30-50 car-length preview distance. While this is appropriate for human drivers, this was excessive for a control implementation and resulted in very slow rise times observed in the previous study.

To complete the vehicle model description, it is useful to add additional scaling transforms to limit the largest control effort, tracking error, and reference input to all have unity 1-norms. To do this, one uses a variable transformation suggested by [16]. For the vehicle system, reasonable signal norms are:

$$\begin{aligned} u_{max} &= 0.1745[rad](=10[degrees]) \\ e_{max} &= 0.15[m](=0.5[scale\ lanes]) \\ r_{max} &= 0.15[m] \end{aligned} \tag{17}$$

Which become in the nondimensional space:

$$\begin{aligned} u^*_{max} &= 0.1745[unitless] \\ e^*_{max} &= \frac{e_{max}}{L} = 0.4184[unitless] \\ r^*_{max} &= \frac{r_{max}}{L} = 0.4184[unitless] \end{aligned} \tag{18}$$

With the signals normalized as above, the goal is to maintain an output position within [-1,1], using control inputs bounded by [-1,1], given a reference input that remains within [-1,1].

4. PERTURBATION DESCRIPTION

Of the original data set of vehicle parameters, only 50 vehicles have been recorded with complete sets of bicycle-model parameters. This subset is hereafter referred to a **V**, and each set member will be referred to as $\mathbf{V_i}$. To specify the average vehicle in the set, the pi values of Equation (3) are calculated at a velocity such that $\pi_3 = 0.5$. This pi-term must be fixed as it cooresponds to the velocity scheduling parameter. The value of 0.5 was chosent somewhat arbitrarily, and it corresponds to 3.0 m/s scale speed or approximately 42 mph for a full-sized vehicle. The nondimensional transfer function for the nominal system is given by:

$$\frac{\bar{y}(s^*)^*}{\delta_f(s^*)} = \frac{1}{s^{*2}} \frac{2.2465 \cdot s^{*2} + 2.9609 \cdot s^* + 1.1563}{s^{*2} + 2.1923 \cdot s^* + 1.5797} \tag{19}$$

Note that $s \Rightarrow s^*$ because s has dimensions of $1/t$ and must also be normalized. With signal normalization as described previously, the transfer function becomes:

$$\begin{aligned} \frac{\hat{\bar{y}}_n^*(s^*)}{\delta_f(s^*)} &= \frac{\bar{y}^*(s^*)}{\delta_f(s^*)} \cdot \frac{u^*_{max}}{e^*_{max}} \\ &= \frac{1}{s^{*2}} \frac{0.9546 \cdot s^{*2} + 1.2582 \cdot s^* + 0.4913}{s^{*2} + 2.1923 \cdot s^* + 1.5797} \end{aligned} \tag{20}$$

A key insight of this work is to utilize the observed variations in Π parameters in database **V** to describe the expected variation of any vehicle controller. The advantage of this approach is that each set of parameters in the database are correctly cross-correlated, thus avoiding the conservatism of one-at-a-time variable manipulation. Additionally, a controller design that is robust to the wide variations in vehicles in **V** should be portable vehicle-to-vehicle.

From the data in database **V**, we compare the relative error between the average vehicle and each individual database member. The frequency-dependent error, e(*jw*), between the average plant and the i[th] plant is given by:

$$e(jw) = \left| \frac{G(jw, \Pi_{1i}, \ldots, \Pi_{5i}) - G(jw, \bar{\Pi}_1, \ldots, \bar{\Pi}_5)}{G(jw, \bar{\Pi}_1, \ldots, \bar{\Pi}_5)} \right| \tag{21}$$

Where *G(jw)* represents the frequency response of the vehicle bicycle model dependent on the Π parameters. A simple multiplicative uncertainty description is used to describe this system variation, represented in block-diagram form in Fig. 3.

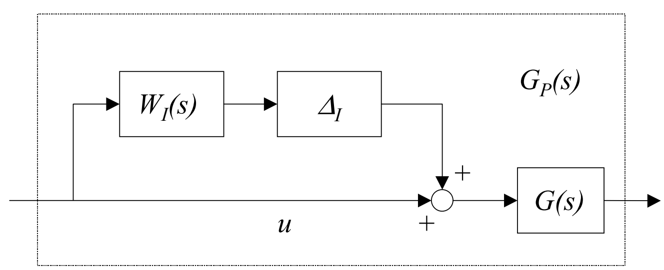

Fig. 3: Multiplicative uncertainty model

The plot of each plant deviation, calculated from (21) for each $\mathbf{V_i}$ in the database **V** is shown in Fig. 4. It is clear that the maximum multiplicative uncertainty is approximately constant over nearly the entire frequency range, a result that justifies a multiplicative representation.

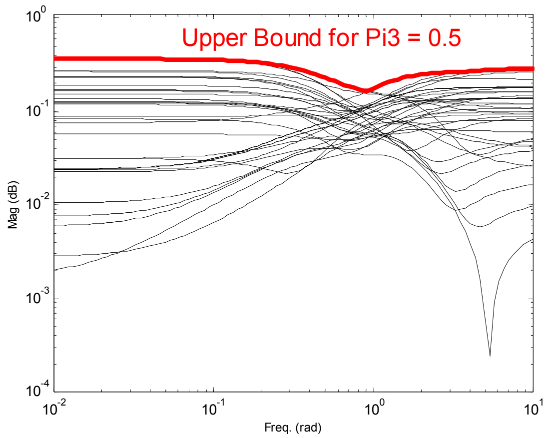

Fig. 4: Multiplicative uncertainty, by frequency

The weight representing system robustness, w_I, is specified by fitting the upper bound of all observed perturbations. In this case:

$$w_I(s^*) = \frac{0.2 \cdot s^* + 0.5}{0.1 \cdot s^* + 1} \tag{22}$$

The high frequency gain was made slightly higher than needed in order to account for possible unmodeled dynamics that are unaccounted for by the bicycle model, such as steering actuator dynamics, vehicle roll and pitch, aerodynamics, etc. The feasibility of the control synthesis problem requires that the uncertainty weighting of Eq. (22) not be too high, and in very high speed or low cornering stiffness cases, this requirement is violated. These limiting cases are discussed extensively in [7, 10].

5. CONTROLLER SYNTHESIS

Because the H-infinity system representation does not allow unstable open-loop systems, the double integrator is approximated with poles very close to the jw-axis:

$$\frac{\bar{y}_n^*(s^*)}{\delta_f(s^*)} \approx \frac{1}{(s^*+K)^2} \frac{0.9546 \cdot s^{*2} + 1.2582 \cdot s^* + 0.4913}{s^{*2} + 2.1923 \cdot s^* + 1.5797} \tag{23}$$

with K = 0.0001. The resulting high DC gain approximates the integrator effect.

The H-infinity controller must balance the tradeoff between three frequency domain criteria: performance weighting, represented by $w_P \cdot S$; control effort, represented by $w_u \cdot KS$; and model uncertainty, represented by $w_I \cdot T$. These three design goals are represented approximately by minimization of the stacked H-infinity norm of [16]:

$$\|N\|_\infty = \left\| \begin{matrix} w_P \cdot S \\ w_u \cdot KS \\ w_I \cdot T \end{matrix} \right\|. \tag{24}$$

Additionally, an exogenous disturbance is added to allow for disturbance rejection in the common case when the steering input may be biased, or where there is a steady disturbance acting on the vehicle such as a road bank angle [17]. The control problem is represented diagrammatically in Fig. 5.

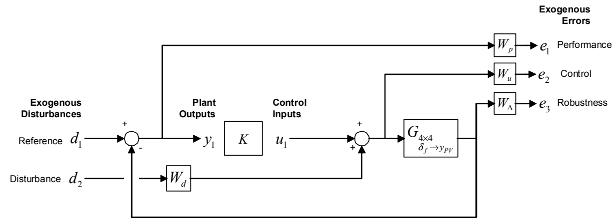

Fig. 5: Classical form of the mixed-sensitivity H-infinity synthesis problem

While w_I was defined in the previous section, the remaining weights, w_P and w_U, represent design variables. In each of the following weighting functions, M_i is the high frequency gain, A_i is the steady-state gain, and w_{Bi} is the approximate crossover bandwidth. The performance weight is given by:

$$w_P(s^*) = \frac{(1/\sqrt{M_P} \cdot s^* + w_{BP})^2}{(s^* + w_{BP} \cdot \sqrt{A_P})^2} \tag{25}$$

With parameters M_P = 1.5, with A_P = 0.01, and w_{BP} = 0.1 rad/sec*. For the control weighting:

$$w_U(s^*) = \frac{(1/\sqrt{M_U} \cdot s^* + w_{BU})^2}{(s^* + w_{BU} \cdot \sqrt{A_U})^2} \tag{26}$$

The control weighting was chosen with M_U = 1/100, A_U = 10, and w_{BU} = 200 rad/sec*. Finally, the disturbance weight is given as $w_D(s^*) = 1$.

The H-infinity controller is obtained using standard robust synthesis routines, which solve the control problem by iterating through possible controller representations seeking to minimize the norm of the stacked sensitivity. A solution was found with a norm of 1.0349, but this solution included a fast pole at s*= -2111. Using model reduction by balanced truncation, the remaining dynamic modes were extracted to produce a controller:

$$\frac{U(s^*)}{E(s^*)} = 6.4274 \cdot \frac{(s^*+2004)}{(s^*+158.6)} \frac{(s^*+10)}{(s^*+10.35)} \frac{(s^*+0.1638)}{(s^*+0.01)^2} \cdot \frac{(s^{*2}+0.2421s^*+0.01625)}{(s^{*2}+1.324s^*+0.5169)} \frac{(s^{*2}+2.216s^*+1.562)}{(s^{*2}+15.03s^*+65.06)} \tag{27}$$

where $E(s^*)$ is the error between the reference signal and previewed feedback. The gamma value larger than unity is due to the control effort exceeding the specified bounds at high frequencies, a violation that is not of particular concern.

6. SIMULATION AND EXPERIMENTAL RESULTS

Experimental testing of this H-infinity controller was conducted in both simulation and experimental platforms. The simulation was necessary to represent the full possible range of vehicle plants, while the experimental vehicle is used to introduce real-world plant variations including

Proceedings of the American Control Conference
Denver, Colorado June 4-6, 2003

nonlinearities, unmodeled dynamics, and disturbances that are otherwise ignored in a simulation study.

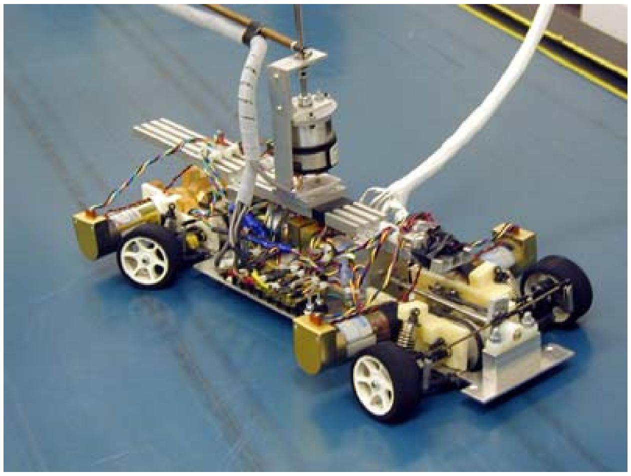

Fig. 6: Experimental test vehicle

The experimental vehicle utilized for testing of the controller is shown in Fig. 6, and the parameters given in Section 2 were measured from this vehicle using methods described in [3, 9]. For the experimental vehicle to operate at a fixed π_3 value of 0.5, it was driven at a speed of 2.95 m/s.

Note that the original generalized controller is designed in nondimensional time and space. For implementation in 'true' space, one must convert the controller into a dimensional form using inverses of the parameter mappings:

$$\left.\frac{U(s)}{E(s)}\right|_{ScaleVehicle} = 142.16 \cdot \frac{u^*_{max}}{e^*_{max}} \cdot \frac{(s+1.619e4)}{(s+1281)} \frac{(s+80.79)}{(s+83.58)} \frac{(s+1.323)}{(s+0.08078)^2} \cdot \frac{(s^2+1.955s+1.061)}{(s^2+10.69s+33.72)} \frac{(s^2+17.9s+101.9)}{(s^2+121.4s+4245)} \quad (28)$$

Note that the signal normalizations from Eq. (17) are also included in the conversion above in variable form. An interesting aspect of the conversion is that the vehicle mass is not needed to transform the generalized nondimensional controller to a specific controller for a particular vehicle.

The vehicle responses from the experimental vehicle are shown in Fig. 7 as the vehicle attempts to track a square wave in lateral position similar to repeated lane change maneuvers. The steering angle was limited to 0.5 radians amplitude due to physical limitations. The H-infinity controller is slightly underdamped, a result that should be expected in consideration of reduced-state feedback combined with severe robustness constraints. Also, there was no system identification outside of measurement of basic parameters: vehicle mass, vehicle length, vehicle velocity, and tire cornering stiffness.

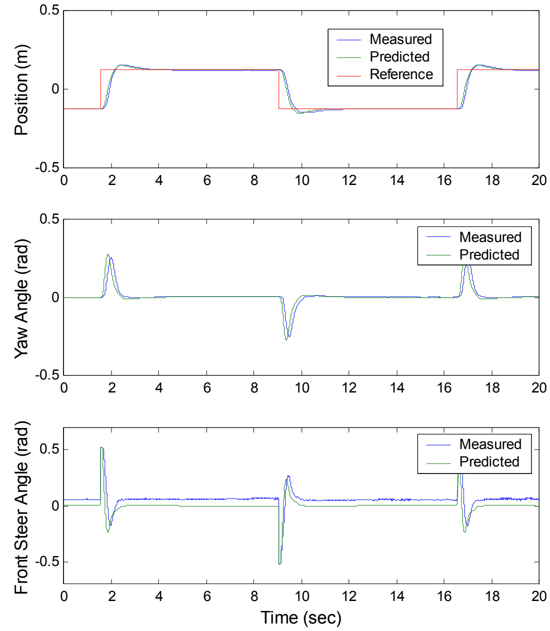

Fig. 7: Experimental closed loop step responses

Also shown in Fig. 7 are the predicted vehicle responses based on a simulation of the linear Bicycle Model with the measured parameters of Section 2. The close match between measured and predicted results shows a good validation of the model for both controller design and for simulation. Even for the aggressive maneuvers above, a very reasonable match is observed between measured and predicted responses.

Using the bicycle model dynamics of the vehicles in the database **V**, the controller was implemented in simulation for each vehicle. The results are shown below. The envelope of responses shows a very reasonable set of vehicle responses for a square-wave tracking problem simulating an emergency lane-change maneuver.

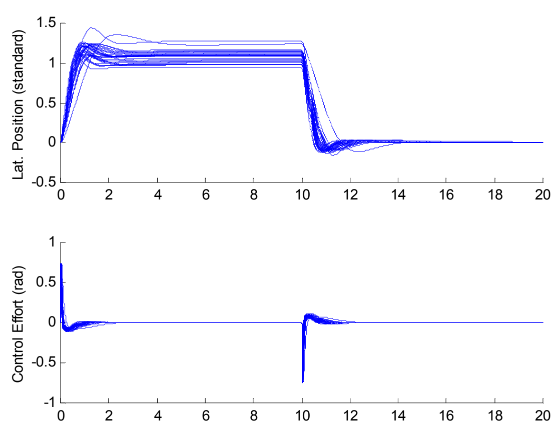

Fig. 8: Simulated Closed-Loop responses for all vehicles in the database

For the responses of Fig. 8, each of the vehicles reach different steady-state values because the amplitude of the square wave was made equal to the vehicle length (in meters), which is different for each vehicle. The larger amplitude responses correspond to longer (and heavier) vehicles. The plots reveal that the larger vehicles are more sluggish in their response, as expected. By nature of using a non-dimensional control formulation, such size effects are implicitly accounted for in the control design.

7. DISCUSSION AND CONCLUSIONS

The key factor limiting the controller performance is the tradeoff between small tracking error, good disturbance rejection, and maintaining system robustness. This well-known tradeoff between robustness and depends on the intent of the control designer. However, it was found that significant tuning could not eliminate the observed overshoot, a fact that is probably due to the coupled nature of the feedback signal. The fixed preview distance forces a fixed ratio between the gain on lateral position and yaw angle.

The difficult problem of attempting to develop a control algorithm suitable for any vehicle was made relatively simple by the use of a generalized, nondimensional control approach. By parameterizing plant dynamics in dimensionless parameters, normal distributions were revealed that intuitively defined an average system. Measured differences between individual vehicles and the average plant motivated a simple multiplicative uncertainty description. An H-infinity methodology based on a stacked sensitivity approach was presented and utilized. Good controller results were obtained in both simulation and on a research vehicle. The research vehicle implementation required minimal identification because the controller, by design, was robust enough to operate nearly any vehicle. Simulated step-responses on a large range of passenger vehicles showed similar results.

REFERENCES

[1] J. Ackermann, "1996 Bode Prize Lecture: Robust Control Prevents Car Skidding," in *IEEE Conference on Decision and Control, June 1996, Reprinted in IEEE Control Systems Magazine, June 1997*, 1996, pp. 23-31.

[2] T. e. a. Tagawa, "Robust Active Steering System Taking Account of Nonlinear Dynamics," *Vehicle System Dynamics Supplement*, vol. 25, pp. 668-681, 1996.

[3] S. Brennan and A. Alleyne, "Robust Stabilization of a Generalized Vehicle, a Nondimensional Approach," presented at 5th International Symposium on Advanced Vehicle Control (AVEC), University of Michigan, Ann-Arbor, 2000.

[4] S. Horiuchi, N. Yuhara, and A. Takei, "Two Degree of Freedom H-infinity Controller Synthesis for Active Four Wheel Steering Vehicles," *Vehicle System Dynamics Supplement*, vol. 25, pp. 275-292, 1996.

[5] E. Ono, K. Takanami, N. Iwama, Y. Hayashi, Y. Hirano, and Y. Satoh, "Vehicle Integrated Control for Steering and Traction Systems by Mu-Synthesis," *Automatica*, vol. 30, pp. 1639-1647, 1994.

[6] J. Sun, A. W. Olbrot, and M. P. Polis, "Robust Stabilizations and Robust Performance Using Model Reference Control and Modeling Error Compensation," *IEEE Transactions on Automatic Control*, vol. 39, pp. 630-635, 1994.

[7] S. Brennan and A. Alleyne, "H-infinity Vehicle Control Using NonDimensional Perturbation Measures," presented at 2002 American Control Conference, Anchorage, Alaska, 2002, pp. 2534–2539.

[8] E. Buckingham, "On Physically Similar Systems; Illustrations of the use of dimensional equations," *Physical Review*, vol. 4, pp. 345-376, 1914.

[9] S. Brennan and A. Alleyne, "Using a Scale Testbed: Controller Design and Evaluation," in *IEEE Control Systems Magazine*, vol. 21, 2001, pp. 15-26.

[10] S. Brennan, "The Application of Nondimensional Analysis to Dynamic Identification, Modeling, and Control," in *Mechanical and Industrial Engineering*. Urbana: University of Illinois at Urbana-Champaign, 2002.

[11] G. J. Heydinger, R. A. Bixel, W. R. Garrot, M. Pyne, J. G. Howe, and D. A. Guenther, "Measured Vehicle Inertial Parameters - NHTSA's Data Through November 1998," *Society of Automotive Engineers*, vol. SAE Paper No. 930897, 1999.

[12] A. Alleyne, "A Comparison of Alternative Obstacle Avoidance Strategies for Vehicle Control," *Vehicle System Dynamics*, vol. 27, pp. 371-392, 1997.

[13] S. Patwardhan, H.-S. Tan, and J. Guldner, "A General Framework for Automatic Steering Control: System Analysis," presented at Proceedings of the American Control Conference, Albuquerque, NM, 1997. pp. 1598-1602.

[14] H. Peng and M. Tomizuka, "Preview Control for Vehicle Lateral Guidance in Highway Automation," *ASME Journal of Dynamic Systems, Measurement and Control*, vol. 115, pp. 679-686, 1993.

[15] J. Guldner, H. S. Tan, and S. Patwardhan, "Analysis of Automatic Steering Control for Highway Vehicles with Look-Down Lateral Reference Systems," *Vehicle System Dynamics*, vol. 26, pp. 243-269, 1996.

[16] S. Skogestad and I. Postlethwaite, *Multivariable Feedback Control, Analysis and Design*. Chichester: Wiley, 1996.

[17] H. E. Tseng, "Dynamic Estimation of Road Bank Angle," *Vehicle System Dynamics*, vol. 36, pp. 307-328, 2001.